Article:

Richardson, TB, Forster, PM orcid.org/0000-0002-6078-0171, Andrews, T et al. (13 more authors) (2018) Carbon dioxide physiological forcing dominates projected Eastern Amazonian drying. Geophysical Research Letters, 45 (6). pp. 2815-2825. ISSN 0094-8276

https://doi.org/10.1002/2017GL076520

Carbon dioxide physiological forcing dominates projected Eastern Amazonian drying

T. B. Richardson[1], P. M. Forster[1], T. Andrews[2], O. Boucher[3], G. Faluvegi[4], D. Fläschner[5], M. Kasoar[6], A. Kirkevåg[7], J.-F. Lamarque[8], G. Myhre[9], D. Olivié[7], B. H. Samset[9], D. Shawki[6], D. Shindell[10], T. Takemura[11], A. Voulgarakis[6]

[1]University of Leeds, Leeds, United Kingdom

[2]Met Office Hadley Centre, United Kingdom

[3]Institut Pierre-Simon Laplace, Université Pierre et Marie Curie / CNRS, Paris, France

[4] NASA Goddard Institute for Space Studies and Center for Climate Systems Research, Columbia University, New York, USA

[5] Max-Planck-Institut für Meteorologie, Hamburg, Germany

[6] Imperial College London, London, United Kingdom

[7] Norwegian Meteorological Institute, Oslo, Norway

[8] NCAR/UCAR, Boulder, USA

[9] CICERO Center for International Climate and Environmental Research – Oslo, Norway

[10] Duke University, Durham, USA

[11] Kyushu University, Fukuoka, Japan

Corresponding author: Thomas Richardson (t.b.richardson@leeds.ac.uk)

Key Points:

- Increased carbon dioxide consistently drives reduced eastern and central Amazonian precipitation in global climate models.
- Projected Amazonian precipitation changes are dominated by the carbon dioxide physiological effect.
- Highlights importance of reducing uncertainties associated with vegetation schemes.

Abstract

Future projections of east Amazonian precipitation indicate drying, but they are uncertain and poorly understood. In this study we analyse the Amazonian precipitation response to individual atmospheric forcings using a number of global climate models. Black carbon is found to drive reduced precipitation over the Amazon due to temperature-driven circulation changes, but the magnitude is uncertain. CO_2 drives reductions in precipitation concentrated in the east, mainly due to a robustly negative, but highly variable in magnitude, fast response. We find that the physiological effect of CO_2 on plant stomata is the dominant driver of the fast response due to reduced latent heating, and also contributes to the large model spread. Using a simple model we show that CO_2 physiological effects dominate future multi-model mean precipitation projections over the Amazon. However, in individual models temperature-driven changes can be large, but due to little agreement, they largely cancel out in the model-mean.

1 Introduction

The Amazon rainforest accounts for 40% of global tropical forest area [Aragão et al., 2014] and plays an important role in the global carbon cycle [Malhi et al., 2006]. Amazonian vegetation and carbon balance are sensitive to changes in precipitation patterns [Phillips et al., 2009; Gatti et al., 2014; Hilker et al., 2014]. However, observed trends and future projections of Amazonian precipitation are highly uncertain [Fu et al., 2013; Joetzjer et al., 2013; Orlowsky and Seneviratne, 2013; Duffy et al., 2015].

Observations suggest an increasing trend in drought conditions [Li et al., 2008], and lengthening of the dry season [Fu et al., 2013], but also a stronger wet season [Gloor et al., 2013]. Future projections from the Coupled Model Intercomparison Project Phase 5 (CMIP5) indicate drying [Boisier et al., 2015], but the inter-model spread is large [Joetzjer et al., 2013]. It is difficult to disentangle which drivers are responsible for the projected changes and associated uncertainties. Various factors could influence Amazonian precipitation, including rising temperatures [Joetzjer et al., 2013; Boisier et al., 2015], land-use change [Spracklen and Garcia-Carreras, 2015; Alves et al., 2017] and fast responses to atmospheric forcing agents [Andrews et al., 2010a; Samset et al., 2016]. Fast precipitation responses can occur on timescales of days to weeks due to the near-instantaneous impact on the atmospheric energy budget [Mitchell et al., 1987; Lambert and Faull, 2007; Andrews et al., 2010b], and can produce significant regional changes [Bony et al., 2013; Richardson et al., 2016; Samset et al., 2016].

CO_2 causes fast precipitation changes not only due to radiative effects, but also due to effects on plant stomata [Cao et al., 2009; Andrews et al., 2010a]. Higher CO_2 concentrations reduce stomatal opening, decreasing evapotranspiration. This is known as the CO_2 physiological effect [Field et al., 1995; Betts, A. R. et al., 1997]. Around 30% of Amazonian precipitation is thought to be fuelled by terrestrial evapotranspiration [Brubaker et al., 1993; Van Der Ent et al., 2010]. Given the high level of vegetation and water recycling, the CO_2

physiological effect could strongly affect Amazonian precipitation, as highlighted in previous studies [Andrews et al., 2010a; Pu and Dickinson, 2014; Abe et al., 2015; Chadwick et al., 2017; Skinner et al., 2017]. However, the precipitation response is uncertain and poorly understood.

To improve understanding of Amazonian precipitation we analyse a range of climate simulations from the Precipitation Driver Response Model Intercomparison Project (PDRMIP) and CMIP5, isolating the response to a variety of forcing agents (CO_2, CH_4, SO_4, black carbon (BC) and insolation (SOL)) and examining the role of fast versus slow responses. Using CMIP5 simulations we isolate the physiological effects of CO_2 on Amazonian precipitation from a multi-model perspective. We construct a simple model for estimating Amazonian precipitation change to establish the main driver of projected changes for the end of the 21st century.

2 Data and Methods

2.1 Precipitation Response to Forcing

Using output from ten climate models participating in PDRMIP (see Table S1-3 and [Myhre et al., 2017]) we analyse the precipitation response to five abrupt global forcing scenarios: doubling CO_2 concentration (2xCO2), tripling methane concentration (3xCH4), ten times BC concentration or emissions (10xBC), five times sulphate concentration or emissions (5xSO4), and a two percent increase in insolation (2%SOL). Perturbations are relative to present-day or pre-industrial values. Simulations were performed with sea surface temperatures (SSTs) fixed for 15 years, and with a coupled ocean for 100 years. Responses are calculated by subtracting a control run from perturbed runs. The PDRMIP models include stomatal conductance sensitivity to CO_2.

We separate the precipitation response into a forcing-dependent fast component and a temperature-driven slow component [Andrews et al., 2010b]. The fast component is taken as the mean response in fixed-SST simulations, in which temperature-driven feedbacks are inhibited. The slow response is calculated using equation 1:

$$\delta P_{slow} = \delta P_{tot} - \delta P_{fast} \quad (1)$$

where δP_{slow} is the slow component, δP_{tot} is the total response (taken as the mean response in the final 50 years of the ocean-coupled simulations), and δP_{fast} is the fast component.

2.2 Energy and Moisture Budget Changes

To understand the precipitation responses we analyse the local atmospheric energy and moisture budgets which provide constraints on precipitation as shown in equation 2:

$$L\delta P = \delta LWC - \delta SWA - \delta SH + \delta H = \delta LH + L\delta M, \quad (2)$$

where L is the latent heat of condensation, P is local precipitation, LWC is net atmospheric longwave radiative cooling, SWA is net atmospheric shortwave absorption, SH is sensible heat flux from the surface, H is dry static energy (DSE) flux divergence, LH is latent heat flux from the surface, M is moisture convergence, and δ represents a perturbation between climates. δH and δM are calculated as residuals. H is driven by changes in horizontal and vertical winds and DSE gradients. In the tropics horizontal DSE gradients are small, therefore changes in H are indicative of changes in vertical motions or the vertical temperature profile of the atmosphere [*Muller and O'Gorman*, 2011].

2.3 CO_2 Physiological Effect

Output from 12 CMIP5 models (Table S5) is used to isolate the CO_2 physiological effect on precipitation. Two sets of experiments (Table S4) are analysed in which SSTs are fixed, and atmospheric CO_2 quadrupled. One set includes physiological effects (sstClim and sstClim4xCO2) and one set does not (amip and amip4xCO2) [Taylor et al., 2011]. The sstClim simulations include a sensitivity of stomatal conductance to CO_2 concentration which determines the evapotranspiration flux (Table S6). In amip simulations either the terrestrial carbon cycle is switched off or vegetation does not see the increase in CO_2.

The response for each set of experiments is calculated by differencing the perturbed run (sstClim4xCO2 or amip4xCO2) and respective control run (sstClim or amip). We then isolate the physiological effects by differencing the two sets of experiments. Although baseline SSTs also differ between experiments, the precipitation changes are shown to be driven locally, suggesting SSTs have little effect. Not all models performed both sstClim and amip experiments. Consistent results are obtained when using only models which performed both (Fig. S1).

2.4 Projected Precipitation Change

Based on the PDRMIP 2xCO2 simulations, we construct a simple model to estimate the contribution of CO_2 and increasing temperature to projected Amazonian precipitation change by the end of the 21st century (2081-2100). For each PDRMIP model we compute an R factor for CO_2, which is the fast precipitation response per unit global-mean TOA forcing, and a hydrological sensitivity (HS), which is the slow precipitation response per unit global-mean temperature change, as shown in equations 3 and 4:

$$R = \delta P_{fast}/F_{CO2} \tag{3}$$

$$HS = \delta P_{slow}/(\delta T_{tot} - \delta T_{fsst}) \tag{4}$$

where, δP_{fast} and δP_{slow} are the fast and slow precipitation responses to doubling CO_2 (see section 2.1 for fast, slow and total definitions), F_{CO2} is global-mean TOA CO_2 forcing, δT_{tot} is the total global-mean surface temperature response, and δT_{fsst} is the global-mean surface temperature response in the fixed-SST simulations (due to land surface). We then use the PDRMIP multi-model mean R and HS to estimate precipitation change following two Representative Concentration Pathways, RCP4.5 and RCP8.5, as shown in equation 5:

$$\delta P(t) = (R_{PDRMIP} \times F_{CO2}(t)) + (HS_{PDRMIP} \times \delta T(t)), \tag{5}$$

where, δP is precipitation change at time t, R_{PDRMIP} is the PDRMIP multi-model mean R factor, F_{CO2} is global-mean TOA CO_2 forcing at time t, HS_{PDRMIP} is the PDRMIP multi-model mean HS, and δT is global-mean surface temperature change at time t. F_{CO2} values are taken from

Meinshausen et al. [2011], and δT is taken as the CMIP5 multi-model mean for the years 2081-2100. CMIP5 precipitation and temperature projections are calculated using output from 15 models (Table S5) which include CO_2 physiological effects. Equation 5 is used to estimate precipitation change for the region-mean shown in Figure 1a, and spatially by calculating R and HS for each gridpoint.

3 Results and Discussion

3.1 Precipitation response to forcing

We first look at the Amazonian precipitation response to individual forcings using the PDRMIP model ensemble (Fig. 1). Doubling CO_2 reduces precipitation over much of the Amazon, in particular the central and eastern regions (Fig. 1a). Conversely, along the north-western edge of South America precipitation increases. The models exhibit good agreement on reduced precipitation in the northeast. However, the magnitude of change, and how far it extends west is variable.

Increasing BC also drives considerable drying over the Amazon (Fig. 1d), with 80% of models agreeing on reductions over much of northern South America. 3xCH4, 5xSO4 and 2%SOL produce only small changes in the central and eastern Amazon (Fig. 1b, 1c, 1e). Sulphate and solar forcing affect precipitation more in the west, with increased insolation enhancing precipitation, and increased sulphate causing drying.

Figure 1f shows the mean precipitation responses for the region outlined in 1a, encompassing eastern and central Amazonia (ECA). The responses are split into contributions from the forcing-dependent fast response, and temperature-driven slow response (temperature responses shown in Fig. S2). The ECA region-mean responses to 3xCH4, 5xSO4 and 2%SOL are small, though inter-model spread is large. The negligible precipitation response to SO_4 and solar forcing arises due to opposing fast and slow terms. Increased SO_4 produces a negative fast response, mainly due to reduced DSE flux divergence (Fig. S3a). This can be explained by reduced downwelling shortwave radiation at the surface, which reduces the land-sea temperature contrast, reducing convection and precipitation over land [Chadwick et al., 2014; Richardson et al., 2016]. The opposite effect occurs for solar forcing. The slow response counteracts these changes; increasing precipitation as global temperatures decrease due to SO_4, and decreasing precipitation as the climate warms due to solar forcing. The model-mean slow response is negative per unit temperature change for all scenarios except 3xCH4, but the magnitude varies (Fig S3b).

Increased CO_2 drives a large reduction in precipitation over the ECA region. The response is dominated by the fast component (-91.1 ± 90.6mm yr^{-1}), compared to the slow (-19.9 ± 104.4mm yr^{-1}). Despite considerable model spread, the negative fast response is very consistent, with 90% of models agreeing on sign. Although the fast component dominates the model-mean, the slow component often contributes significantly in individual models. In 50% of models the temperature-driven responses are larger than the fast component, but there is little agreement on sign.

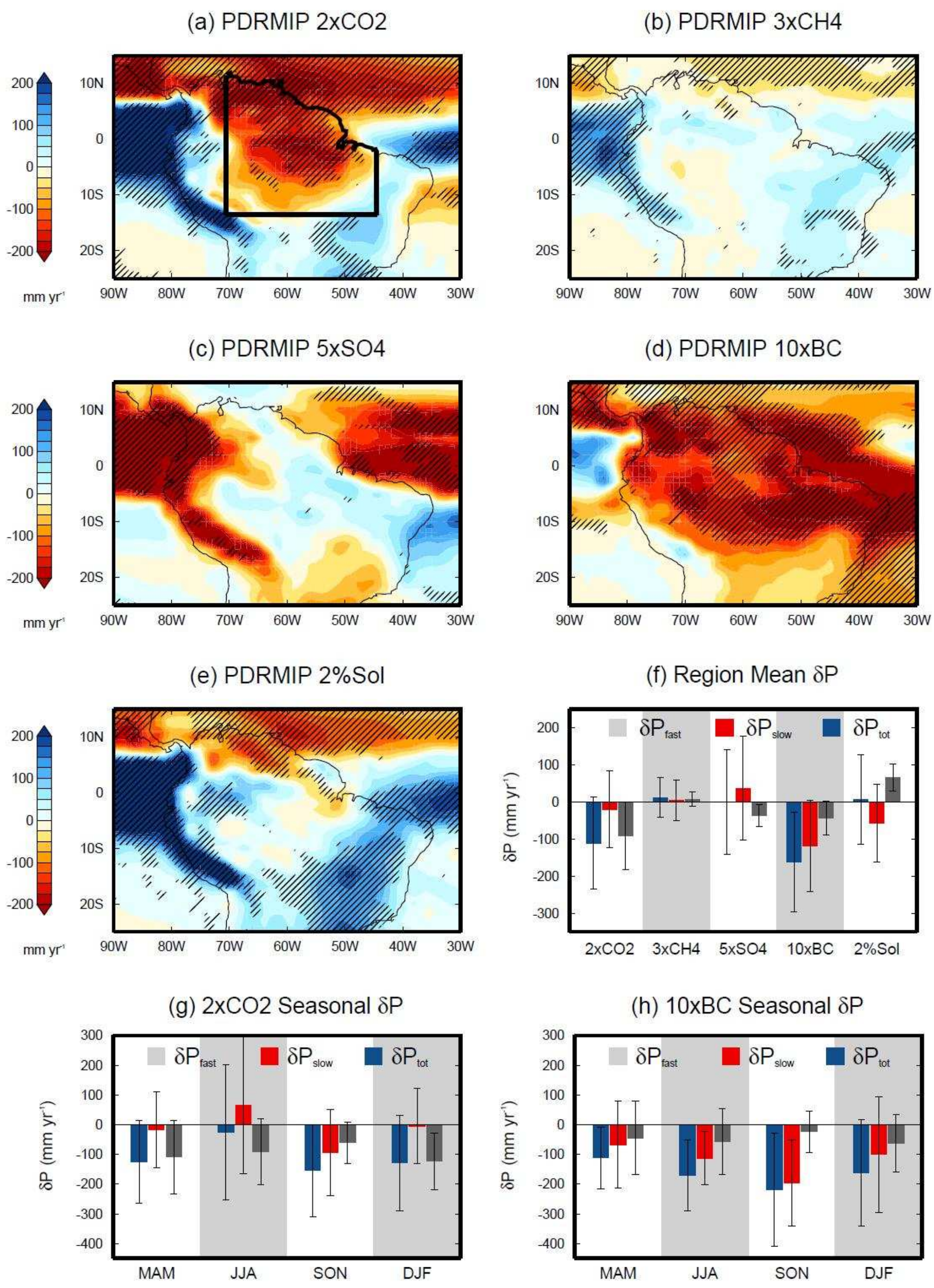

Figure 1: PDRMIP multi-model mean total precipitation response to (a) 2xCO2, (b) 3xCH4, (c) 5xSO4, (d) 10xBC and (e) 2%SOL. Hatching denotes where 80% of models agree on sign of change. Panel (f) shows the PDRMIP multi-model mean precipitation response for the ECA region outlined in panel (a). Total response shown in blue, fast component in grey, and slow component in red. Panels (g) and (h) show the seasonal response to 2xCO2 and 10xBC. Error bars denote model spread standard deviation.

Increased BC drives reduced precipitation over the ECA region. The model-mean response to 10xBC is dominated by the temperature-driven response (-118.3 ± 122.3mm yr^{-1}), rather than the fast component (-44.0 ± 45.3mm yr^{-1}). The inter-model spread is large, but the sign of change is robust across models.

Figure 1g shows the seasonal breakdown of the ECA region-mean 2xCO2 precipitation response. The slow response causes reduced SON precipitation, indicating a strengthening of the late dry season. Previous studies have shown future projections suggest a strengthened and longer dry season [Joetzjer et al., 2013; Boisier et al., 2015]. However, the slow response also enhances JJA precipitation, resulting in little annual-mean change. The fast response drives reduced precipitation throughout the year, with the largest reduction during the wet season.

BC drives larger reductions in precipitation during the dry season (Fig. 1h), when higher levels of biomass burning occur in South America. Hodnebrog et al. [2016] similarly found that BC most strongly affects precipitation in South Africa during the dry season.

3.2 Energy and moisture budget changes

To understand the mechanisms driving the ECA region-mean precipitation response to CO_2 and BC we analyse the energy and moisture budgets (Fig. 2). The negative CO_2 fast response arises mainly due to repartitioning of sensible and latent heat fluxes, as well as reduced LW cooling (Fig. 2a). CO_2 strongly affects surface heat fluxes, reducing LH and increasing SH. The changes in surface fluxes are caused by physiological effects (see section 3.3). The changes in horizontal heat and moisture transport, associated with circulation, are very uncertain. The LH response also exhibits considerable inter-model spread, and is highly correlated with the fast precipitation response inter-model spread (r = 0.92). Given that both evapotranspiration and precipitation decrease, the change in surface runoff (P-E, equivalent to M) is relatively small (-21.8 ± 51.1mm yr^{-1}).

The negative fast precipitation response to BC is driven by increased atmospheric shortwave absorption (Fig. 2c). The uncertainty largely arises from the circulation response, with changes in moisture convergence contributing strongly to inter-model spread (r^2 = 0.90).

The slow response to 2xCO2 is small due to counteracting energy budget feedbacks (Fig. 2b). LW cooling increases with warming, which is countered by increased SW absorption, increased SH, and reduced divergence of DSE flux. The LW and SW radiative feedbacks per unit Kelvin are fairly consistent across forcing scenarios (Fig. S3). The different slow precipitation responses across forcings largely arise from the SH feedbacks.

For 2xCO2, changes in horizontal DSE and moisture fluxes are very uncertain (Fig. 2b), and contribute strongly to inter-model spread in the slow precipitation response (r^2 = 0.92 and r^2 = 0.85). Therefore, although the model-mean slow response is small, in individual models temperature-driven circulation changes can drive large changes in precipitation. However, the slow response shows little agreement in sign or magnitude. Circulation changes are known to be important for tropical precipitation patterns [Chou et al., 2009; Seager et al., 2010; Chadwick et al., 2013]. Future circulation changes are uncertain and may be strongly influenced by chaotic natural variability and model errors [Shepherd, 2014].

Despite causing a weak global temperature response, 10xBC produces a large negative slow precipitation response over the Amazon. The slow response is robustly negative, but variable in magnitude. This is mainly driven by circulation changes, indicated by reduced divergence of DSE flux and moisture convergence (Fig. 2d). BC has been shown to drive northward shifts in the inter-tropical convergence zone (ITCZ) in models [Chung and Seinfeld, 2005; Jones et al., 2007; Kovilakam and Mahajan, 2015], due to the forcing asymmetry. The ITCZ shift is evident in the slow precipitation response spatial pattern (Fig. S4). These circulation changes, combined with a repartitioning of LH and SH, drive the negative slow precipitation response. However, it should be noted that the 10xBC perturbation is large. If the total precipitation response is linearly scaled based on TOA forcing to present-day levels (1981-2000) relative to pre-industrial, the response reduces to -25.9 ± 8.3mm yr^{-1}.

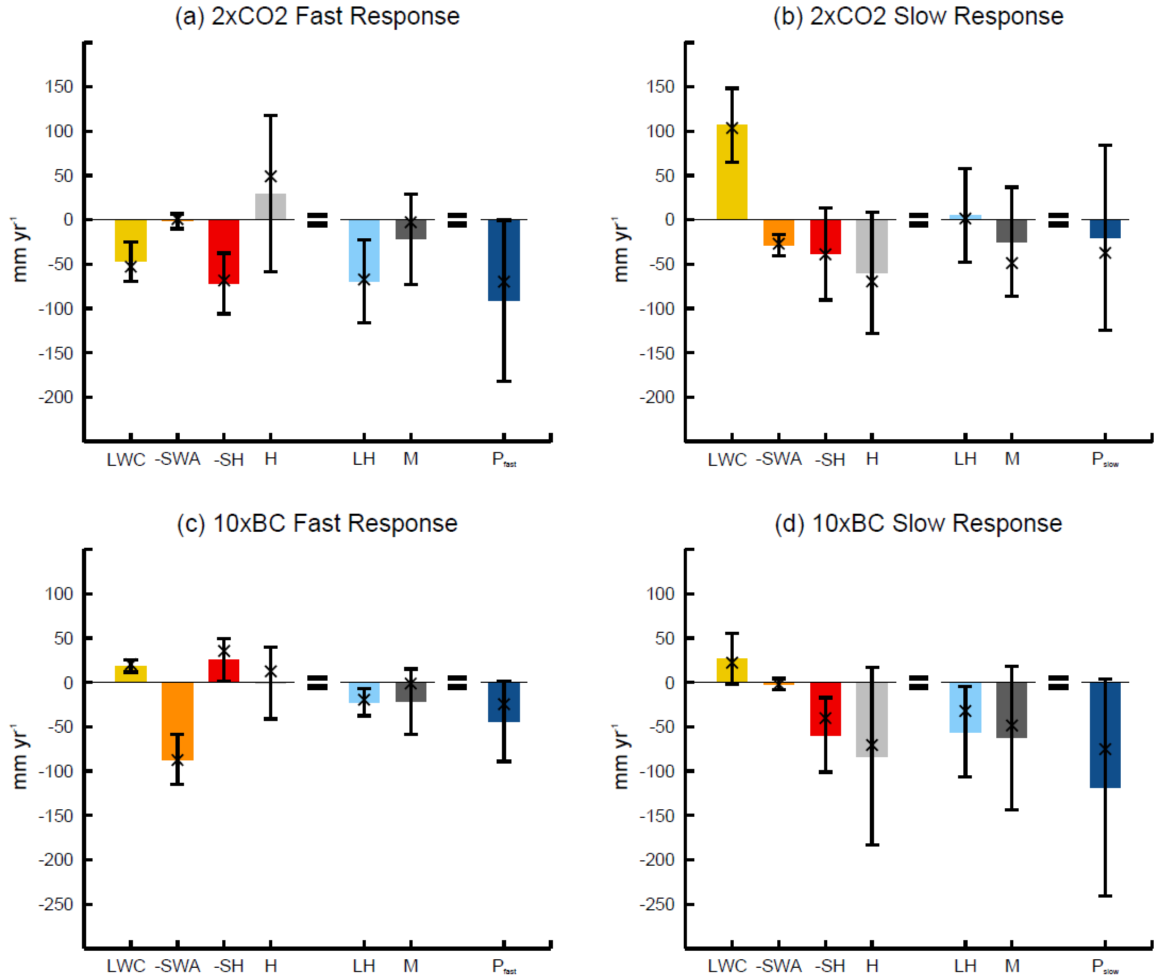

Figure 2: PDRMIP multi-model mean precipitation, energy and moisture budget (see Equation 2) responses to (a, b) 2xCO2 and (c, d) 10xBC, split into (a, c) fast and (b, d) slow components, for the ECA region. Signs for terms are given according to Equation 2. Crosses indicate the median and error bars denote model spread standard deviation.

The largest increases in BC occur over Asia [Myhre et al., 2017]. However, the large changes in BC over Asia drive very little change in Amazonian precipitation (Fig. S5), indicating local biomass burning emissions drive the response.

3.3 CO_2 physiological effect

Figure 3 shows the role of physiological effects on plants in driving the fast precipitation response to CO_2 by comparing CMIP5 sstClim4xCO2 simulations (include physiological effects) and amip4xCO2 simulations (do not include physiological effects). In the amip4xCO2 simulations multi-model mean precipitation increases over most of tropical South America. In contrast, in the sstClim4xCO2 simulations drying extends much further inland from the east. Figure 3c shows the difference between scenarios. Over much of the Amazon, particularly in the east, CO_2 physiological effects drive considerable drying. In contrast, along the west coast precipitation is enhanced. The multi-model mean response is generally in agreement with previous single-model studies [Andrews et al., 2010a; Pu and Dickinson, 2014; Abe et al., 2015; Skinner et al., 2017].

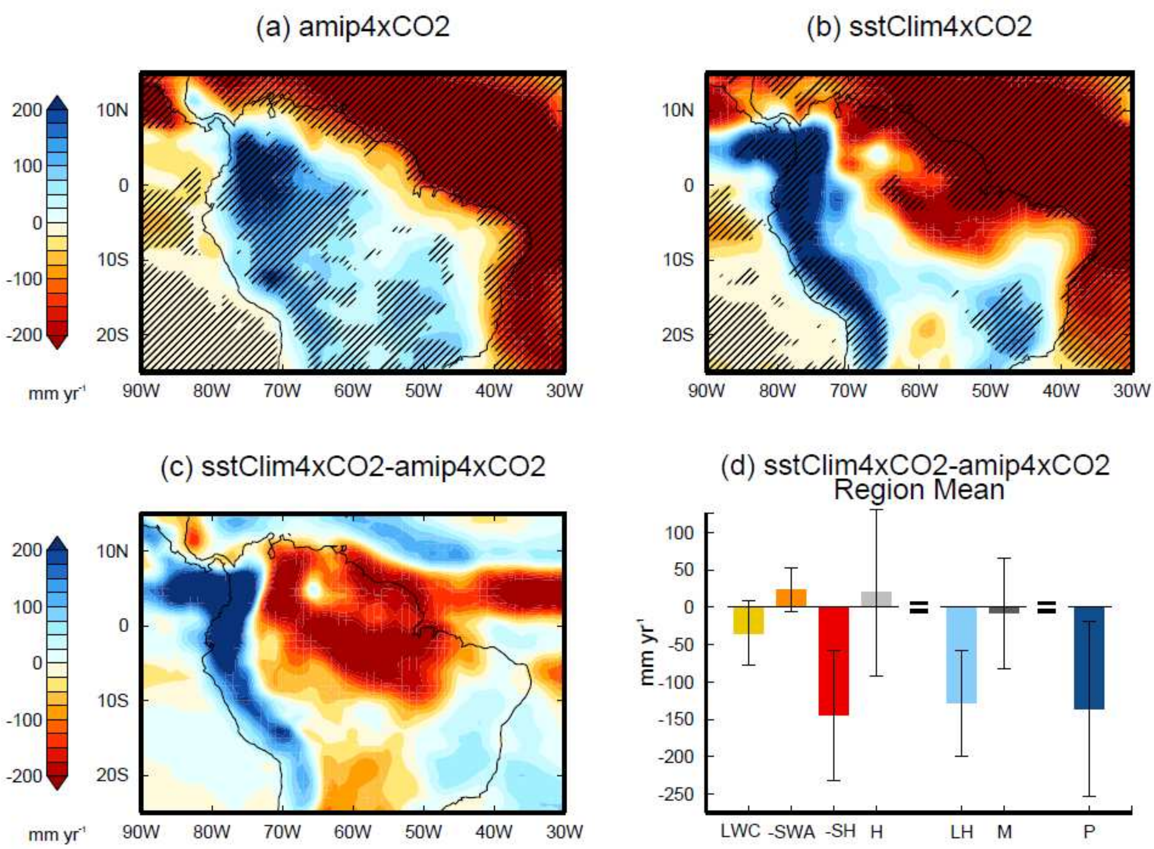

Figure 3: CMIP5 multi-model mean precipitation response to quadrupling CO_2 in (a) amip and (b) sstClim simulations and (c) the difference. Hatching shows where 80% of models agree on sign of change (not applicable in panel (c)). Panel (d) shows the difference between sstClim and amip energy and moisture budget responses for the ECA region. Error bars denote the model spread standard deviation.

Figure 3d shows the physiological effects on energy and moisture budgets for the ECA region. The reduced precipitation due to CO_2 physiological forcing is almost entirely due to repartitioning of sensible and latent heat fluxes. Increased CO_2 reduces stomatal conductance [Field et al., 1995], reducing evapotranspiration. In the Amazon, where water recycling is important [Zemp et al., 2014], the reduction in evapotranspiration drives considerable drying. Surface energy balance is maintained through increased SH flux. There is very little change in horizontal heat and moisture fluxes, indicating the importance of local changes.

The strongest reductions in precipitation occur in the eastern and central Amazon. This may be because the evaporation recycling ratio (fraction of local evaporation which returns as local precipitation) is higher in the east [Van Der Ent et al., 2010]. The increase in precipitation along the west coast is consistent with Skinner et al. [2017], who found that decreased evapotranspiration warms the land-surface and draws moisture from the nearby ocean, increasing convective instability and heavy rainfall events.

The CO_2 physiological effect also drives a large fraction of the fast precipitation response uncertainty for the ECA region. The inter-model standard deviation in the sstClim4xCO2 simulations (109mm yr^{-1}) is over double that for amip4xCO2 (42mm yr^{-1}). Including CO_2 physiological effects considerably increases the uncertainty in latent and sensible heat flux responses (Fig. S6), which contribute strongly to the large model spread. In addition, the uncertain response of surface heat fluxes leads to more uncertainty in the horizontal transport of energy and moisture. This is consistent with studies which have shown uncertainty in transpiration sensitivity contributes strongly to uncertainty in the global-mean fast precipitation response to CO_2 [DeAngelis et al., 2016] and future projections of terrestrial precipitation [Mengis et al., 2015].

3.4 Projected precipitation change

We have shown that the reduction in precipitation over central and eastern Amazonia in response to CO_2 is dominated by the fast component, which is driven by physiological effects on evapotranspiration. Therefore, given that CO_2 forcing increasingly dominates in future emission scenarios [van Vuuren et al., 2011], the CO_2 physiological effect could play a key role in projections. To quantify the potential contribution of CO_2 to precipitation change over the Amazon by the end of the 21st century we construct a simple model based on the PDRMIP results. Precipitation change over the Amazon is estimated by scaling the fast component based on CO_2 TOA forcing for the end of the century, and scaling the slow component based on global-mean surface temperature change (Eq. 5). The simple model is compared with CMIP5 multi-model mean projections, calculated using 15 models (Table S5) which include physiological effects [Collins et al., 2013], in Figure 4.

The CMIP5 projections indicate drying over large areas of the Amazon particularly in the east, south and north. In contrast, along the west coast of South America precipitation increases. Changes are larger for RCP8.5, following a business as usual emissions scenario, but the spatial pattern is very similar. Despite the large predicted changes, there is considerable variation across models. Over tropical South America there are very few regions in which more than 80% of models agree on the sign of change. Although agreement on the spatial pattern is low, models consistently project large changes [Chadwick et al., 2015].

The simple model predicts a similar drying (-151.1 ± 82mm yr^{-1}) over the ECA region as CMIP5 projections (-160.9 ± 241mm yr^{-1}) following RCP8.5, driven almost entirely by the fast response to CO_2. For RCP4.5 the simple model predicts more drying (-87.1 ± 47mm yr^{-1}) than CMIP5 projections (-34.5 ± 120mm yr^{-1}). The comparison suggests that projected drying in the ECA region is predominantly driven by CO_2 physiological forcing. Therefore, projected drying is independent of increasing temperatures, as supported by the lack of correlation between global-mean warming and precipitation change across CMIP5 models (r = 0.16 and -0.09 for RCP4.5 and RCP8.5).

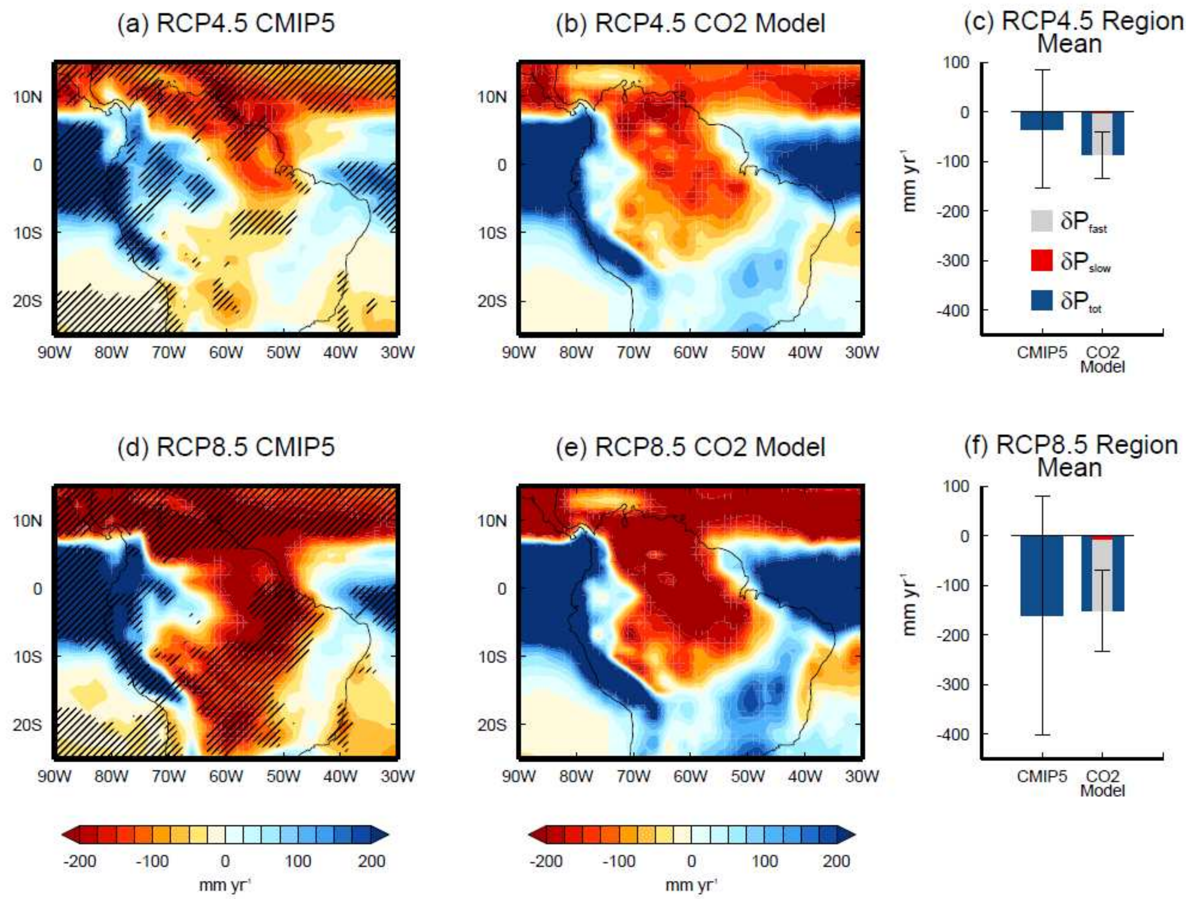

Figure 4: Projected precipitation change for 2081-2100 relative to pre-industrial, following (a, b, c) RCP4.5 and (d, e, f) RCP8.5, calculated using (a, d) CMIP5 multi-model mean (only models which include CO_2 physiological effects) and (b, e) the simple model given by Equation 5. Hatching denotes where 80% of models agree on sign of change. Panels (c) and (f) show mean change for the ECA region. Total change in blue, the fast component in grey and slow component in red. Error bars denote the standard deviation of CMIP5 model spread, and the standard error of the simple model.

Spatially there are very similar features between the simple model and CMIP5 projections. These include significant drying over the eastern, southern and northern Amazon, and increased precipitation in the west, all of which are predominantly driven by the fast response to CO_2 (Fig. S7). There are some notable differences, such as in the western Amazon, where enhanced precipitation extends further east in CMIP5 projections. This may be due to drivers not included in the simple model, such as land-use change, aerosols, and greenhouse gases other than CO_2. Land-use change is likely to be the most influential forcing not included [Spracklen and Garcia-Carreras, 2015], and may account for the difference between the simple model and CMIP5 projections for the ECA region-mean under RCP4.5.

The simple model indicates that CO_2 physiological forcing could dominate multi-model mean future projections of precipitation change over large areas of the Amazon. However, individual models show that temperature-driven circulation changes can be large, but are highly uncertain and show little agreement.

4 Conclusions

We have presented the Amazonian precipitation response to individual atmospheric forcings using the PDRMIP model ensemble. Precipitation changes exhibit considerable inter-model spread, but there are some robust signals. Increased BC drives a robust drying over the Amazon, however the magnitude of change varies across models. The reduction in precipitation is largely due to temperature-driven circulation changes, associated with a northward shift in the ITCZ. The fast precipitation response to BC also contributes to drying due to enhanced SW absorption.

Increased CO_2 concentrations drive reduced Amazonian precipitation, particularly in the east. The model-mean drying is dominated by the fast component, for which 90% of models agree on reduced precipitation over the ECA region. Using CMIP5 model output we find that physiological effects dominate the fast response to CO_2 over the Amazon, through a change in partitioning of sensible and latent heat fluxes. Higher CO_2 concentrations reduce stomatal opening and consequently evapotranspiration. This limits moisture availability and precipitation over much of the Amazon, particularly in the east. Physiological effects also drive increased precipitation along the west coast. Physiological effects contribute strongly to the uncertainty in Amazonian precipitation changes, over doubling the inter-model spread for the ECA region.

Using a simple model based on CO_2 TOA forcing and global-mean surface temperature change we quantify the potential contribution of CO_2 to precipitation changes over the Amazon by the end of the century (2081-2100) relative to pre-industrial. The simple model suggests that CMIP5 multi-model mean projected drying over the ECA region is predominantly driven by CO_2 physiological effects. This implies projected Amazonian precipitation change is independent of rising temperatures, being mainly driven by atmospheric CO_2 concentration. However, it should be noted that temperature-driven changes can be large in individual models, but show little agreement. Our findings illustrate the importance of short-timescale processes on long-term precipitation change in this region, and highlight the need to reduce uncertainties associated with vegetation schemes.

Acknowledgements

CMIP5 and PDRMIP model output is publicly available for download (see http://pcmdi9.llnl.gov and http://www.cicero.uio.no/en/PDRMIP/PDRMIP-data-access, respectively). T.B.R. was supported by a NERC CASE award in collaboration with the Met Office NE/K007483/1 and NERC grant NE/N006038/1. P.M.F. was supported by a Royal Society Wolfson Merit Award and NERC grant NE/N006038/1. T.A. was supported by the Newton Fund through the Met Office Climate Science for Service Partnership Brazil (CSSP Brazil). B.H.S. and G.M. were funded by the Research Council of Norway, through the grant NAPEX (229778). D.S. and G. F. thank NASA GISS for funding and acknowledge the NASA High-End Computing Program through the NASA Center for Climate Simulation at Goddard Space Flight Center for computational resources. O.B. acknowledges HPC resources from TGCC under the gencmip6 allocation provided by GENCI (Grand Equipement National de Calcul Intensif). T.T. is supported by the NEC SX-ACE supercomputer system of the National Institute for Environmental Studies, Japan, the Environmental Research and Technology Development Fund (S-12-3) of the Ministry of Environment, Japan and JSPS KAKENHI Grant Numbers JP15H01728 and JP15K12190. M.K., D.S. and A.V. were supported by the Natural Environment Research Council under grant NE/K500872/1, and from the Grantham Institute at Imperial College. Simulations with HadGEM2 and HadGEM3-GA4 were performed using the MONSooN system, a collaborative facility supplied under the Joint Weather and Climate Research Programme, which is a strategic partnership between the Met Office and the Natural Environment Research Council. D.O. and A.K. were supported by the Norwegian Research Council through the projects EVA (grant 229771), EarthClim (207711/E10), NOTUR (nn2345k), and NorStore (ns2345k)

References

Abe, M., H. Shiogama, T. Yokohata, S. Emori, and T. Nozawa (2015), Asymmetric impact of the physiological effect of carbon dioxide on hydrological responses to instantaneous negative and positive CO2 forcing, Clim. Dyn., 45(7–8), 2181–2192, doi:10.1007/s00382-014-2465-1.

Alves, L. M., J. A. Marengo, R. Fu, and R. J. Bombardi (2017), Sensitivity of Amazon Regional Climate to Deforestation, Am. J. Clim. Chang., 6(1), 75–98, doi:10.4236/ajcc.2017.61005.

Andrews, T., M. Doutriaux-Boucher, O. Boucher, and P. M. Forster (2010a), A regional and global analysis of carbon dioxide physiological forcing and its impact on climate, Clim. Dyn., 36(3–4), 783–792, doi:10.1007/s00382-010-0742-1.

Andrews, T., P. M. Forster, O. Boucher, N. Bellouin, and A. Jones (2010b), Precipitation, radiative forcing and global temperature change, Geophys. Res. Lett., 37(14), n/a-n/a, doi:10.1029/2010GL043991.

Aragão, L. E. O. C., B. Poulter, J. B. Barlow, L. O. Anderson, Y. Malhi, S. Saatchi, O. L. Phillips, and E. Gloor (2014), Environmental change and the carbon balance of Amazonian forests, Biol. Rev., 89(4), 913–931, doi:10.1111/brv.12088.

Betts, A. R., Cox, P. M., and S. E. Lee (1997), Contrasting Physiological and Structural Vegetation Feedbacks in Climate Change Simulations, Nature, 387(June), 796–799, doi:10.1038/42924.

Boisier, J. P., P. Ciais, A. Ducharne, and M. Guimberteau (2015), Projected strengthening of Amazonian dry season by constrained climate model simulations, Nat. Clim. Chang., 5(7), 656–660, doi:10.1038/nclimate2658.

Bony, S., G. Bellon, D. Klocke, S. Sherwood, S. Fermepin, and S. Denvil (2013), Robust direct effect of carbon dioxide on tropical circulation and regional precipitation, Nat. Geosci., 6(6), 447–451, doi:10.1038/ngeo1799.

Brubaker, K. L., D. Entekhabi, and P. S. Eagleson (1993), Estimation of continental precipitation recycling, J. Clim., 6(6), 1077–1089, doi:10.1175/1520-0442(1993)006<1077:EOCPR>2.0.CO;2.

Cao, L., G. Bala, K. Caldeira, R. Nemani, and G. Ban-Weiss (2009), Climate response to physiological forcing of carbon dioxide simulated by the coupled Community Atmosphere Model (CAM3.1) and Community Land Model (CLM3.0), Geophys. Res. Lett., 36(10), 1–5, doi:10.1029/2009GL037724.

Chadwick, R., I. Boutle, and G. Martin (2013), Spatial Patterns of Precipitation Change in CMIP5: Why the Rich Do Not Get Richer in the Tropics, J. Clim., 26(11), 3803–3822, doi:10.1175/JCLI-D-12-00543.1.

Chadwick, R., P. Good, T. Andrews, and G. Martin (2014), Surface warming patterns drive tropical rainfall pattern responses to CO 2 forcing on all timescales, Geophys. Res. Lett., 41(2), 610–615, doi:10.1002/2013GL058504.

Chadwick, R., P. Good, G. Martin, and D. P. Rowell (2015), Large rainfall changes consistently projected over substantial areas of tropical land, Nat. Clim. Chang., (September), 1–6, doi:10.1038/nclimate2805.

Chadwick, R., H. Douville, and C. B. Skinner (2017), Timeslice experiments for understanding regional climate projections: applications to the tropical hydrological cycle and European winter circulation, Clim. Dyn., 0(0), 1–19, doi:10.1007/s00382-016-3488-6.

Chou, C., J. D. Neelin, C.-A. Chen, and J.-Y. Tu (2009), Evaluating the “Rich-Get-Richer” Mechanism in Tropical Precipitation Change under Global Warming, J. Clim., 22(8), 1982–2005, doi:10.1175/2008JCLI2471.1.

Chung, S., and J. Seinfeld (2005), Climate response of direct radiative forcing of anthropogenic black carbon, *J. Geophys. Res. ...*, 110(D11), D11102, doi:10.1029/2004JD005441.

Collins, M. et al. (2013), Long-term Climate Change: Projections, Commitments and Irreversibility, Clim. Chang. 2013 Phys. Sci. Basis. Contrib. Work. Gr. I to Fifth Assess. Rep. Intergov. Panel Clim. Chang., 1029–1136, doi:10.1017/CBO9781107415324.024.

DeAngelis, A. M., X. Qu, and A. Hall (2016), Importance of vegetation processes for model spread in the fast precipitation response to CO_2 forcing, Geophys. Res. Lett., 1–10, doi:10.1002/2016GL071392.

Duffy, P. B., P. Brando, G. P. Asner, and C. B. Field (2015), Projections of future meteorological drought and wet periods in the Amazon, Proc. Natl. Acad. Sci., 112(43), 13172–13177, doi:10.1073/pnas.1421010112.

Van Der Ent, R. J., H. H. G. Savenije, B. Schaefli, and S. C. Steele-Dunne (2010), Origin and fate of atmospheric moisture over continents, Water Resour. Res., 46(9), 1–12, doi:10.1029/2010WR009127.

Field, C. B., R. B. Jackson, and H. A. Mooney (1995), Stomatal responses to increased CO2: implications from the plant to the global scale, Plant, Cell Environ., 18(10), 1214–1225, doi:10.1111/j.1365-3040.1995.tb00630.x.

Fu, R. et al. (2013), Increased dry-season length over southern Amazonia in recent decades and its implication for future climate projection, Proc. Natl. Acad. Sci., 110(45), 18110–18115, doi:10.1073/pnas.1302584110.

Gatti, L. V et al. (2014), Drought sensitivity of Amazonian carbon balance revealed by atmospheric measurements, Nature, 506(7486), 76–80, doi:10.1038/nature12957.

Gloor, M., R. J. W. Brienen, D. Galbraith, T. R. Feldpausch, J. Schöngart, J. L. Guyot, J. C. Espinoza, J. Lloyd, and O. L. Phillips (2013), Intensification of the Amazon hydrological cycle over the last two decades, Geophys. Res. Lett., 40(9), 1729–1733, doi:10.1002/grl.50377.

Hilker, T., A. I. Lyapustin, C. J. Tucker, F. G. Hall, R. B. Myneni, Y. Wang, J. Bi, Y. Mendes de Moura, and P. J. Sellers (2014), Vegetation dynamics and rainfall sensitivity of the Amazon, Proc. Natl. Acad. Sci., 111(45), 16041–16046, doi:10.1073/pnas.1404870111.

Hodnebrog, Ø., G. Myhre, P. M. Forster, J. Sillmann, and B. H. Samset (2016), Local biomass burning is a dominant cause of the observed precipitation reduction in southern Africa, Nat. Commun., 7, 11236, doi:10.1038/ncomms11236.

Joetzjer, E., H. Douville, C. Delire, and P. Ciais (2013), Present-day and future Amazonian precipitation in global climate models: CMIP5 versus CMIP3, Clim. Dyn., 41(11–12), 2921–2936, doi:10.1007/s00382-012-1644-1.

Jones, A., J. M. Haywood, and O. Boucher (2007), Aerosol forcing, climate response and climate sensitivity in the Hadley Centre climate model, J. Geophys. Res., 112(July), D20211, doi:10.1029/2007JD008688.

Kovilakam, M., and S. Mahajan (2015), Black carbon aerosol-induced Northern Hemisphere tropical expansion, Geophys. Res. Lett., 42(12), 4964–4972, doi:10.1002/2015GL064559.

Lambert, F. H., and N. E. Faull (2007), Tropospheric adjustment: The response of two general circulation models to a change in insolation, Geophys. Res. Lett., 34(3), L03701, doi:10.1029/2006GL028124.

Li, W., R. Fu, R. I. N. Juárez, and K. Fernandes (2008), Observed change of the standardized precipitation index, its potential cause and implications to future climate change in the Amazon region., Philos. Trans. R. Soc. Lond. B. Biol. Sci., 363(1498), 1767–72, doi:10.1098/rstb.2007.0022.

Malhi, Y. et al. (2006), The regional variation of aboveground live biomass in old-growth Amazonian forests, Glob. Chang. Biol., 12(7), 1107–1138, doi:10.1111/j.1365-2486.2006.01120.x.

Meinshausen, M. et al. (2011), The RCP greenhouse gas concentrations and their extensions from 1765 to 2300, Clim. Change, 109(1), 213–241, doi:10.1007/s10584-011-0156-z.

Mengis, N., D. P. Keller, M. Eby, and A. Oschlies (2015), Uncertainty in the response of transpiration to CO_2 and implications for climate change, Environ. Res. Lett., 10(9), 94001, doi:10.1088/1748-9326/10/9/094001.

Mitchell, J., C. Wilson, and W. Cunnington (1987), On CO₂ climate sensitivity and model dependence of results, Q. J. R. Meteorol. Soc., 113(475), 293–322, doi:10.1256/smsqj.47516.

Muller, C. J., and P. a. O'Gorman (2011), An energetic perspective on the regional response of precipitation to climate change, Nat. Clim. Chang., 1(5), 266–271, doi:10.1038/nclimate1169.

Myhre, G. et al. (2017), PDRMIP: A Precipitation Driver and Response Model Intercomparison Project—Protocol and Preliminary Results, Bull. Am. Meteorol. Soc., 98(6), 1185–1198, doi:10.1175/BAMS-D-16-0019.1.

Orlowsky, B., and S. I. Seneviratne (2013), Elusive drought: Uncertainty in observed trends and short-and long-term CMIP5 projections, Hydrol. Earth Syst. Sci., 17(5), 1765–1781, doi:10.5194/hess-17-1765-2013.

Phillips, O. L. et al. (2009), Drought Sensitivity of the Amazon Rainforest, Science (80-.)., 323(5919), 1344–1347, doi:10.1126/science.1164033.

Pu, B., and R. E. Dickinson (2014), Hydrological changes in the climate system from leaf responses to increasing CO2, Clim. Dyn., 42(7–8), 1905–1923, doi:10.1007/s00382-013-1781-1.

Richardson, T. B., P. M. Forster, T. Andrews, and D. J. Parker (2016), Understanding the Rapid Precipitation Response to CO 2 and Aerosol Forcing on a Regional Scale*, J. Clim., 29(2), 583–594, doi:10.1175/JCLI-D-15-0174.1.

Samset, B. H. et al. (2016), Fast and slow precipitation responses to individual climate forcers: A PDRMIP multi-model study, Geophys. Res. Lett., n/a-n/a, doi:10.1002/2016GL068064.

Seager, R., N. Naik, and G. A. Vecchi (2010), Thermodynamic and dynamic mechanisms for large-scale changes in the hydrological cycle in response to global warming, J. Clim., 23(17), 4651–4668, doi:10.1175/2010JCLI3655.1.

Shepherd, T. G. (2014), Atmospheric circulation as a source of uncertainty in climate change projections, Nat. Geosci., 7(10), 703–708, doi:10.1038/ngeo2253.

Skinner, C. B., C. J. Poulsen, R. Chadwick, N. S. Diffenbaugh, and R. P. Fiorella (2017), The Role of Plant CO_2 Physiological Forcing in Shaping Future Daily-Scale Precipitation, J. Clim., 30(7), 2319–2340, doi:10.1175/JCLI-D-16-0603.1.

Spracklen, D. V., and L. Garcia-Carreras (2015), The impact of Amazonian deforestation on Amazon basin rainfall, Geophys. Res. Lett., 42(21), 9546–9552, doi:10.1002/2015GL066063.

Taylor, K. E., R. J. Stouffer, and G. a Meehl (2011), A Summary of the CMIP5 Experiment Design, , 4(January 2011), 1–33.

van Vuuren, D. P. et al. (2011), The representative concentration pathways: An overview, Clim. Change, 109(1), 5–31, doi:10.1007/s10584-011-0148-z.

Zemp, D. C., C. F. Schleussner, H. M. J. Barbosa, R. J. Van Der Ent, J. F. Donges, J. Heinke, G. Sampaio, and A. Rammig (2014), On the importance of cascading moisture recycling in South America, Atmos. Chem. Phys., 14(23), 13337–13359, doi:10.5194/acp-14-13337-2014.